PHYSICAL REVIEW VOLUME 183, NUMBER 1 5 JULY 1969

Attenuation and Lifetime of Hot Electrons Injected into Liquid Helium

David G. Onn and M. Silver
Department of Physics, University of North Carolina, Chapel Hill, North Carolina, 27514
(Received 20 February 1969)

We have obtained current densities up to 10^{-9} A cm^{-2} by injection of hot electrons from a cold-cathode emitter into liquid helium. The current in helium is only 1% of that available from the same devices into vacuum at liquid-helium temperatures. The current attenuation has been explained in terms of the electron-helium barrier, the back diffusion of the quasifree nonlocalized electrons near the emitter surface, and the thermalization of the quasifree electrons to a localized state while still within the influence of their image potential due to the emitter surface. Using a model based on these three factors the lifetime of the quasifree electrons has been calculated. In the present experiments the lifetime has varied from 2.5 psec, for the lowest helium densities and highest energy electrons to 0.3 psec for the reverse conditions.

I. INTRODUCTION

Over the past few years, a great deal of evidence, both experimental and theoretical, has indicated that the negative ion in liquid helium consists of a self-trapped electron in a "bubble" or cavity.[1-4] The bubble structure is favored energetically over the quasifree, or nonlocalized, electron because of the strong repulsive interaction between an electron and a helium atom.[5] This repulsive interaction has been investigated theoretically[6-8] and experimentally.[9] Estimated values of the bubble radius are generally between 10 and 20 Å.[3,10-12] A determination of the bubble radius for the similar problem of positronium in liquid helium gives the value 21 Å at 4.2°K.[13]

A further effect of the strong electron-helium repulsion is the presence of a potential barrier at the surface of liquid helium opposing the injection of electrons into the bulk of the liquid. This barrier has been calculated based on several models of liquid helium,[3-14] the values obtained lying between 0.5 and 1.5 eV. Several experiments have been carried out to determine the barrier directly. Sommers[15] used an electron gun to inject electrons directly through the free surface of liquid helium and obtained a value of 1.3 eV, though this method requires assumptions of the energy distribution of the electrons in the low-pressure helium gas immediately above the liquid surface. Woolf and Rayfield[16] used a commercial photocathode and obtained a value of 1.08 eV, but the current they observed in the liquid helium was only 10^{-6} of that obtained from the cathode in vacuum. This large attenuation is as yet unexplained.

Recent work by Zipfel and Sanders[17] shows that the energy required to excite the electron out of the bubble at 1.3°K is about 0.65 eV, increasing with pressure to a value greater than 1 eV at the same temperature.

None of the above experiments on the barrier were carried out above the λ point. Due to the low heat generated by cold cathodes, however, it is possible to use them to carry out injection experiments above the λ point. The electron-helium barrier is a function of the helium density, and although the density can be changed by the application of pressure, a larger change is possible by increasing the temperature up to the critical point. We have previously reported injection from cold-cathode emitters into liquid helium.[18] The value of the barrier (2–3 eV) obtained from early experiments was much larger than any reported previously. Further experiments[19] have shown that this value arose from irregular operation of the cold-cathodes emitters, and oversimplification of the injection phenomena. The latter criticism applies also to all work on electron injection into liquid helium to date.

The work reported in this paper is an extension of the earlier experiments on injection of electrons into liquid helium from cold-cathode emitters.[18,19] It has proved possible to reconcile the main features of the experimental injection data with a model for the injection process for an electron entering liquid helium. This model takes into account the existence of the surface barrier, and the behavior of the electron in its initial quasifree state prior to thermalization into a bubble state.

II. EXPERIMENTAL METHOD

A. Construction and Operation of the Cold-Cathode Emitters

For the purpose of understanding the results of the present work it is convenient to regard the cold-cathode emitter as a gold surface from

which hot electrons are emitted. The emitters used in these experiments were Al-Al_2O_3-Au diodes of the type first described by Mead,[20] and summarized in an excellent review by Crowell and Sze[21] to whom reference should be made for earlier work. This type of emitter was recently studied in detail at room temperature and at 77°K by Savoye and Anderson,[22] though under pulsed operating conditions.

We have found that at 4.2°K stable, long-term operation of these emitters is possible under dc conditions since the current through the diodes is much less than at higher temperatures thus reducing destructive effects in the oxide and the gold surface.

A layer of aluminum, about 2000 Å thick, is evaporated onto a cleaned glass substrate, and the surface oxidized in aqueous solution in the standard manner,[23] to give an oxide layer of known thickness. Estimates of thickness were made from the electrolysis voltage using an average rate of 13 Å per volt. The oxide thickness used is typically between 70 and 150 Å depending on the anticipated operating voltage of the emitter. The edges of the aluminum strip are protected by additional electrolysis. Finally a layer of gold, about 200 Å thin is evaporated at right angles to the aluminum strip, while thick gold contacts are evaporated simultaneously. Generally, three emitters are made on one substrate and are found to have almost identical properties.

The thickness of oxide needed to sustain a given applied emitter voltage was originally determined empirically by sacrificing one emitter out of the three on a substrate. It is well known[22,24] that both the emission current, i_e, and the diode current, i_d, decay with time. At 4.2°K this decay is reduced as higher voltages are applied to the emitter until, above a critical voltage both currents will increase with time to a stable value above the initial value. Ultimately, operated above this critical voltage, both currents become unstable and break down, though this process may take many hours. The relationship of this critical voltage to conditions within the oxide will be discussed elsewhere.[25] If the emitter is kept at least 0.1 V below the critical voltage, both diode current and emission current become quite stable with time, and the emitter will operate for days at 4.2°K. The amount of stability achieved depends on the thickness of the oxide. In general, for thin-oxide emitters good final stability is still difficult to achieve, and correction for aging of the emitted current during a data run must be applied.

Typical operating conditions for an emitter are these: oxide thickness 100 Å; $i_d = 25$ μA; $v_d = 8$ V; $i_e = 10^{-8}$ A. The heat generated is thus about 2mW cm^{-2}, since the active area is 0.1 cm^2. The operating efficiency (i_e/i_d) is 4×10^{-4}. The heat generated is such that the emitter can be operated above the λ point without causing bubbling or excessive turbulence in the liquid helium.[26]

A vacuum characteristic for a typical emitter is shown in Fig. 1. The emitted current, i_e, is plotted against the reciprocal of the emitter driving voltage, v_d. Although emission into vacuum is detectable over a range of about 2 V, data in liquid helium is obtainable only over a range of 1 V or less, since the current is reduced to about 1% of the values shown in Fig. 1, while the sensitivity is still the same.

The energy distribution of the emitted electrons is not easily determined.[27] Experiments are presently under way to characterize the dependence of the energy distribution on emitter driving voltage, gold layer thickness, oxide thickness, and temperature. From past studies, however, we do have enough knowledge of the general nature of the distribution to explain our present injection data. Thus we know that the emitted electrons have energies ranging over a few eV,[27,28] and that the width of the energy distribution, and the average energy can be controlled by the emitter driving voltage.[28,29] We also know that the maximum energy of the emitted electrons cannot exceed ($v_d - \phi_{Au}$).

In the past, attempts have been made to describe the cold-cathode emission by comparison

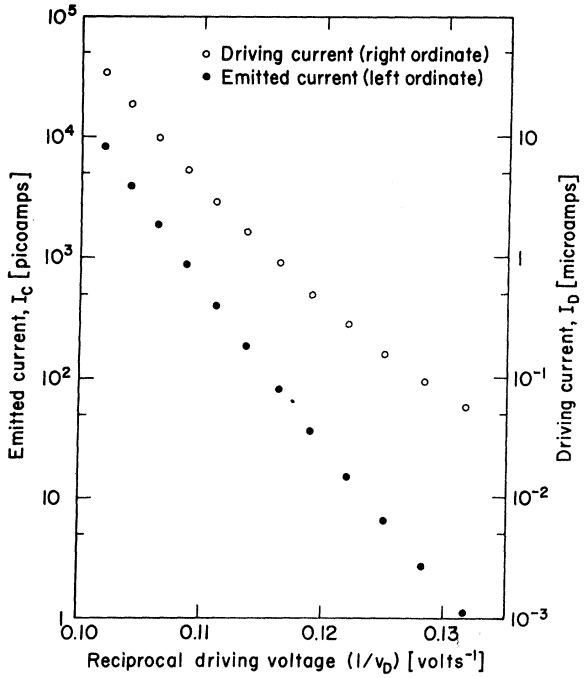

FIG. 1. Typical emitter vacuum characteristic. Collected current (i_c) is plotted as a function of reciprocal emitter driving voltage.

with a hot thermionic emitter, using a Richardson equation

$$I = AT^2 e^{-\phi/kT}, \quad (1)$$

where for the cold emitter, "T" is an "effective temperature" which is proportional to the driving voltage.[30] Though this may be valid at room temperature, the differences in the mode of operation of the emitters at room temperature and at 4.2°K[25] suggest that such a description may not be possible at low temperatures.

B. Circuit and Cryostat

The circuit used is shown in Fig. 2, together with a schematic illustration of the cryostat used. The emitter and collector are mounted inside a container which can be evacuated and immersed in liquid helium in a standard metal Dewar. The container is sealed by an indium O ring. Liquid helium may be admitted by means of a valve mounted below the helium liquid level in the Dewar, and operated from the cryostat head.

The digital voltmeter (DVM) determines the emitter driving voltage v_d to ±2 mv and enables a precise return to any previous operating state. The Keithley 610B Electrometer is used to monitor the diode current, i_d, since this provides a constant check on the state of aging of the emitter.[25] A Keithley 602 Electrometer, capable of operating up to 1500 V off ground is used to measure the current collected from the helium sample. Because of leakage current, due to high voltage leads in the cryostat head, the present limit of detectable current is 0.1 pA, though with improved isolation, the full capabilities of the electrometer will be used. Various emitter-collector spacings have been tested and appear to have no effect on the results obtained. The present spacing of 0.75 mm, combined with the voltage limit on the electrometer enables collector fields across the helium sample up to 20 kV cm^{-1}.

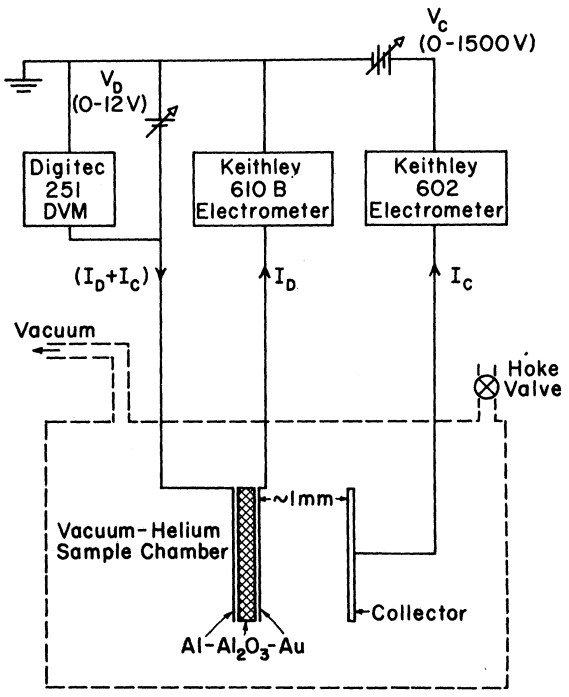

FIG. 2. Circuit diagram and schematic of cryostat. The arrows indicate electron current.

The emitter substrate is thermally grounded to the bath by means of vacuum grease, and no effect due to the heating of the emitter by its own heat generation has been detected. This fact indicates that there is adequate dissipation of heat by the gold and aluminum layers and by the substrate itself, thus further reducing the possibility of bubble formation due to heating of the helium.

The temperature is determined by means of a calibrated germanium resistance thermometer in a four-lead circuit. It is checked for consistency against a mercury manometer on every cooling at 4.2°K and the λ point. The Dewar may be pressurized in order to reach temperatures above 4.2°K, though the size of the present helium sample limits the application of this technique because of lack of equilibrium at higher temperatures. The experiments reported have all been carried out with bath helium, admitted to the sample chamber through a cotton filter. No difference is noted when deliberately dirty helium is used, and although we plan to use specially purified helium in the future, purity does not seem an important factor at present.

III. RESULTS

We have taken data in two forms. Referring to Fig. 2 for the significance of each voltage, we have taken characteristics of (i) collected current i_C versus $(1/v_d)$ with v_C constant (i.e., constant applied field E_A) and (ii) i_C versus E_A with v_d constant. In case (ii) the emitter is acting as a constant current source.

A typical i_C versus $(1/v_d)$ curve is shown in Fig. 3. E_A was maintained at various constant values. For comparison the same characteristic for the emitter operating into vacuum is shown, though with a current scale reduced by a factor of 100. There are two notable features of these characteristics. First, there is a reduction of the current into liquid helium, to about 1% of that into vacuum. Second, the slopes of the data are different for vacuum and helium. We previously attributed this slope difference to the presence of the electron-helium barrier, which

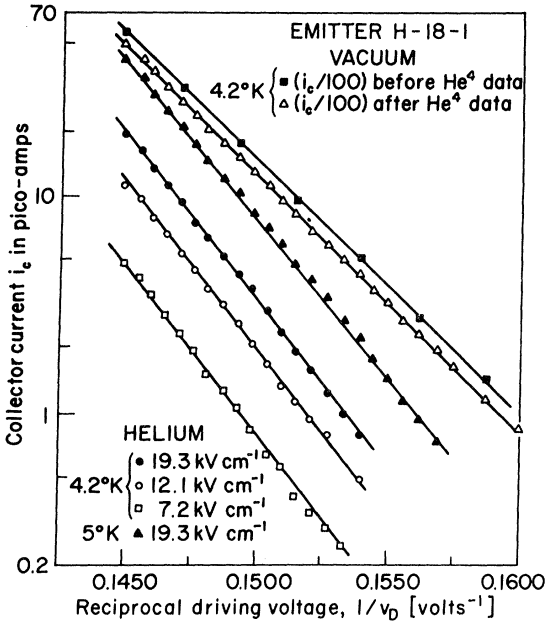

FIG. 3. Comparison of collected current in vacuum and in liquid helium. i_c is plotted as a function of $(1/v_d)$ for various values of the electric field applied to the helium sample.

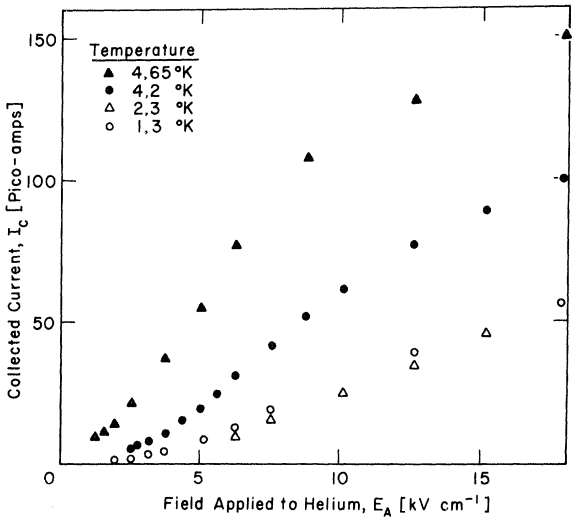

FIG. 4. Collected current in liquid helium plotted against applied field for various helium temperatures. The emitter is operating as a constant current emitter while this data is taken.

would cause a new effective work function, analysis being in terms of Eq. (1). However, as we see below, the use of this analysis at low temperatures is inaccurate. In fact the slope difference can be explained adequately in terms of our model, and is not directly due to the electron-helium barrier. Final interpretation of this slope difference, and its variation with emitter driving voltage must wait upon precise knowledge of the energy distributions of the emitted electrons.

A set of i_C versus E_A characteristics is shown in Fig. 4, where v_d was kept constant, but the helium temperature was changed. The important features of these curves are (a) the currents do not saturate at the highest fields obtainable; (b) the current is strongly dependent on temperature above the λ point; (c) the current reaches a minimum at a given E_A at or near the λ point; then increases slightly with decreasing temperature below the λ point. The variations with temperature will finally be interpreted in terms of changes in density of the liquid helium.

Characteristics similar to Figs. 3 and 4 have been determined for a wide variety of operating conditions, for emitters of oxide thicknesses between 60 and 150 Å. A full description of the results obtained will be reserved for later discussion (Sec. V), when they will be compared with the results expected from the injection model.

IV. THE INJECTION MODEL

A. Diffusion of the Injected Electrons

The model we have proposed is illustrated in Fig. 5. That an electron close to a metal surface is within the influence of its own image potential $(e/2x)$ is well established, from field emission studies, and has been shown to be theoretically consistent.[31] The application of an electric field (E_A) causes a lowering of the work function, ϕ, by an amount

$$e\Delta\phi = e^{3/2}E_A^{1/2}\,. \tag{2}$$

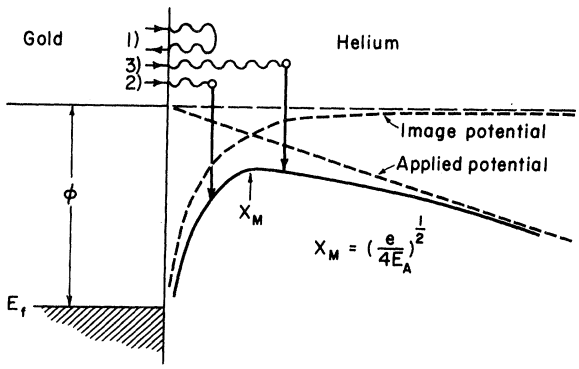

FIG. 5. Schematic of the injection model. For clarity, the electron-helium barrier is suppressed, and ϕ may be taken as the total effective work function.

In addition, there is a peak in the potential experienced by the emitted electron. The position of the peak is a distance x_M from the metal surface, where

$$x_M = (e/4E_A)^{1/2} . \quad (3)$$

The field strengths used in these studies (< 20 kV cm^{-1}) are such that the lowering of the work function is too small to be of consequence. However, the presence of the helium at the gold surface increases the importance of the potential peak since for our field strengths x_M lies between 150 and 1000 Å. These distances are comparable to or greater than the mean free path (m.f.p.) for scattering of electrons in helium.

In a good vacuum, any electron emitted above the work function of gold is collected. We propose that the hot electrons injected from the gold surface of the emitter into liquid-helium scatter from the helium atoms and lose energy to the helium. The fractional energy loss in each collision will depend upon the type of collision. This point will be discussed below in connection with the relevant m.f.p. used to describe the scattering. We assume, however, that the highly mobile, quasifree hot electrons undergo a random walk through the helium with the possibility that at some point thermalization occurs to a less mobile state (probably a bubble state). There are then three possible paths for the electron, illustrated in Fig. 5.

An electron may back diffuse to the emitter, as shown in path (1) without thermalization occurring, causing some reduction in the current collected from the helium. The reduction in current will be independent of the position of the potential peak, and thus of the applied field. This process of back diffusion was discussed in detail by J.J. Thomson[32] and his arguments will be applied in detail to the present case. If the electron does become thermalized, the thermalization may occur as in path (2) in Fig. 5, between the emitter surface and the potential peak, in which case the relatively immobile thermalized electron will return to the emitter causing a further reduction in collected current. If thermalization occurs beyond the potential peak, the electron will be collected by means of the applied field. The reduction of current due to the thermalization process will be dependent on the applied field due to the variation of the position of the potential peak with applied field. The potential peak is providing, in effect, a gate at distance x_M from the emitter surface.

B. Thomson Back Diffusion in Liquid Helium

J. J. Thomson originally discussed back diffusion while considering photoemission into a gas.[32] In that case the electrons rapidly attached to a gas atom to form an ion, and the back diffusion of the ions to the photocathode caused a reduction of the collected current below the vacuum emission current.

In the present case we consider the back diffusion of the injected hot electrons before they become thermalized. In liquid helium there is a high density of scatterers for the incoming electron and we assume a mean free path for scattering, x_χ. The nature of x_χ will be discussed at the end of this section, but for the present we take x_χ to be small (a few Å). The electrons then diffuse in a random-walk process into the helium, and may back diffuse to the emitter before thermalization.

We characterize the incoming hot electrons, after they have overcome the electron-helium barrier, by a velocity c. Since $\epsilon^{1/2} \propto c$, where ϵ is the electron energy, the velocity is not a rapid function of energy.

Following Thomson, if ρ_F is the charge density of quasifree electrons, then the hot-electron current density available within the liquid (J_a) is reduced below the total emitted current density injected (J_{inj}) due to the back-diffusion term

$$J_a = J_{\text{inj}} - c\rho_F/(6\pi)^{1/2} . \quad (4)$$

We consider the quasifree electrons to be thermalized with a characteristic relaxation time, τ, and characteristic range, x_0, so that at equilibrium we can write

$$J_a = \rho_F x_0/\tau \quad (5)$$

and Eq. (4) becomes

$$J_a = J_{\text{inj}}\{1 + c\tau/[x_0(6\pi)^{1/2}]\}^{-1} . \quad (6)$$

If D is the diffusion constant for the quasifree electrons we can use kinetic theory to remove some of the uncertainty arising from the presence of the thermal velocity c in Eq. (6). We can write

$$x_0 = (D\tau)^{1/2} \quad (7)$$

and

$$D = (cx_\chi)/6 , \quad (8)$$

where x_χ is the scattering m.f.p. controlling the diffusion of the quasifree electrons. Then Eq. (6) reduces to

$$I_a = I_{\text{inj}}[1 + (6/\pi)^{1/2}(x_0/x_\chi)]^{-1} , \quad (9)$$

where currents I_a, I_{inj} replace current densities. Thus if we can determine (I_a/I_{vac}) and x_0, we can determine the relevant m.f.p. describing the scattering, x_χ. Now, x_0 can be determined from the field dependence of the current reduction.

However, the electron-helium barrier prevents unambiguous determination of (I_a/I_{vac}) and it becomes necessary to use a reasonable value for x_x in order to determine the relative current reduction contributions of the barrier and the back-diffusion effects.

The recent results of Zipfel and Sanders[17] on the effective electron-helium barrier, determined by excitation of electrons out of their bubble state into the liquid, gives a value of 0.65 eV, which is quite compatible with the value deduced from considering the helium as a collection of independent scattering centers. The relevant m.f.p. is then that for elastic scattering, x_s, which may be determined from

$$x_s = 1/n\sigma , \tag{10}$$

where n is the atomic density of the scattering medium, and σ is the scattering cross section. Using the density of liquid helium at 4.2°K, and the scattering cross section obtained experimentally[9] (which agrees closely with calculated values[6-8]), for electrons scattering from helium gas, we obtain $x_s = 10.8$ Å at 4.2°K. The variation of x_s with temperature is obtained directly from the variation of the liquid-helium density. Both experiment and calculation indicate that the cross section is constant with energy over the range 0.05 to 1 eV, and varies only slowly on the fringes of this range.

The scattering length calculated from the experimental gas-phase determinations of the cross section has been used in past calculations of the helium barrier where, in one case[14] the helium was considered as an effective solid, and, in another case,[5] correlations in the liquid were taken into account. In both cases the barrier obtained was greater than 1 eV, and agreed with earlier experiments,[15,16] but not with the most recent determination of 0.65 eV.

In the following section we will discuss our results assuming that $x_x = x_s$ and point out later what effect other values of the effective mean free path would have. Setting $x_x = x_s$ the Eqs. (7) and (8) enable us to estimate the lifetime, τ, of the quasifree electron before thermalization, since

$$c\tau = 6x_0^2/x_s . \tag{11}$$

Thus, since we can determine x_0, from the field-dependent current reduction we can determine $(c\tau)$. From the energy limits on the electrons available from our emitters we can then set limits on the lifetime of the quasifree electrons. Though this is not necessarily the time for complete formation of the final bubble state, it does give an indication of the time for initiation of the bubble formation, which would consist of a large mobility drop.[4]

C. Thermalization of the Quasifree Electrons

We now examine the thermalization of the quasifree injected electrons, originally highly mobile, to a less mobile thermalized state. Using continuity of current for both the quasifree electrons and the thermalized electrons we obtain

$$-\vec{\nabla}\cdot\vec{J}_F - \rho_F/\tau = 0 , \tag{12}$$

$$-\vec{\nabla}\cdot\vec{J}_T + \rho_F/\tau = 0 , \tag{13}$$

where τ is the characteristic lifetime for relaxation from the quasifree state, subscript F, to the thermalized state, subscript T.

Developing the equation for the quasifree electrons we obtain

$$-\frac{\partial}{\partial x}\left(-D_F\frac{\partial\rho_F}{\partial x} + \rho_F\mu_F E(x)\right) - \frac{\rho_F}{\tau} = 0 , \tag{14}$$

where D_F and μ_F are the diffusion constant and mobility. We are concerned with the current passing beyond the potential peak at x_M (Fig. 5). Solving Eq. (14) in the region near x_M, where $E(x) \simeq 0$ we obtain

$$\rho_F = \rho_{0F}\, e^{-x/x_0} . \tag{15}$$

We are concerned with the current density of the diffusing quasifree electrons at x_M, which is given by

$$J_M = -D_F\left.\frac{\partial\rho_F}{\partial x}\right|_{x=x_M} \tag{16}$$

$$= \left(\frac{D_F}{x_0}\rho_{0F}\right) e^{-x_M/x_0} . \tag{17}$$

Using the results of the previous section on Thomson back diffusion it follows that

$$J_a = \frac{D_F}{x_0}\rho_{0F} , \tag{18}$$

where J_a is the current density available after Thomson back diffusion is taken into account. The current I_c collected beyond x_M can then be written as

$$I_c = I_a\, e^{-(x_M/x_0)} . \tag{19a}$$

Under our present field strength conditions this solution is adequate, though with higher applied fields, where x_M is much closer to the surface, the solution of Eqs. (12) and (13) for the complete field, including the image term, must be made.

A difficulty arises in discussing the energy

losses as the hot electrons are thermalized. If we consider the quasifree electron to be undergoing elastic collisions with mean free path x_s, then the number of collisions in a random walk to a distance x_0 is given by

$$N = x_0^2/x_s^2 \ . \tag{19b}$$

For the values x_0 that we obtain (about 50 to 150 Å) and the values of x_s for the same helium densities N would be between 100 and 400. If the collision is elastic, then the maximum energy lost by the electron in each collision is only about 0.001 of its energy before the collision. An electron with initially 0.5 eV cannot lose all of its energy by the number of elastic collisions occurring in a random walk, and the final loss of energy necessary to achieve thermalization (i.e., only the zero-point energy of the electron in its bubble remaining) must occur in a final inelastic process. Alternatively the energy lost in one collision could be greater, in which case x_s may not be the correct m.f.p. to use. However, as we shall see later in discussing the limits obtained on the possible values of the lifetime for thermalization, the relevant m.f.p. cannot be less than approximately $(x_s/3)$ nor greater than x_0.

Cohen and Lekner[33] recently pointed out that in dense systems there are different m.f.p.'s for energy and momentum transfer for hot electrons moving under a strong steady applied field. However, we cannot at present say which m.f.p. should be used to describe the thermalization process occurring in our experiments, since the electrons enter the helium with an initial energy, and those of greatest consequence undergo thermalization in a very low-field region. A full theoretical study of the thermalization process and the energy losses involved would be extremely useful.

D. The Complete Current Equation

There are two other possible sources for reduction of the injected current below the vacuum level. These are the electron-helium barrier and the transmission coefficient of the metal-liquid helium surface, which may not be the same as that of the metal-vacuum surface. The exact effect of the electron-helium barrier cannot be determined until the exact energy distribution of the emitted electrons is known. Even then this method is not likely to yield a very precise value of the electron-helium barrier since there are three competing effects in the total injection picture. Nevertheless, the general influence of the barrier in reducing the current can be seen. The attenuating effect of the barrier we term A.

There is also a possibility of a change in transmission coefficient due to the detailed shape of the electron-helium barrier, and the unknown effect of the suggested close-packed surface layer[34] on electrons transmitted. The attenuating effect of change of transmission we term T, and combine the barrier term with this term as (AT), since they are not separately determinable at present.

Thus the complete equation for the current collected from the liquid helium in terms of the current available in vacuum becomes, using Eqs. (9), (19a) and setting $x_X = x_s$:

$$I_c = \frac{I_{\text{vac}}(AT)}{1+(6\pi)^{1/2}\, x_0/x_s}\, e^{-x_M/x_0}$$

$$= I_\infty\, e^{-x_M/x_0} \ , \tag{20}$$

where I_∞ is the current available under (unattainable) infinite applied field; $x_M = (e/4E_a)^{1/2}$ and

$$(I_\infty/I_{\text{vac}}) = (AT)[1+(6\pi)^{1/2} x_0/x_s]^{-1} \ . \tag{21}$$

We have shown schematically in Fig. 6 the effect of the various terms in Eq. (21). The figure shows the original vacuum current, I_{vac}, for a fixed v_d, which is independent of the collector field E_A, at least for values of E_A in the range in which we operate. The effect of each term is shown separately, together with the effect of the liquid-helium density on each term.

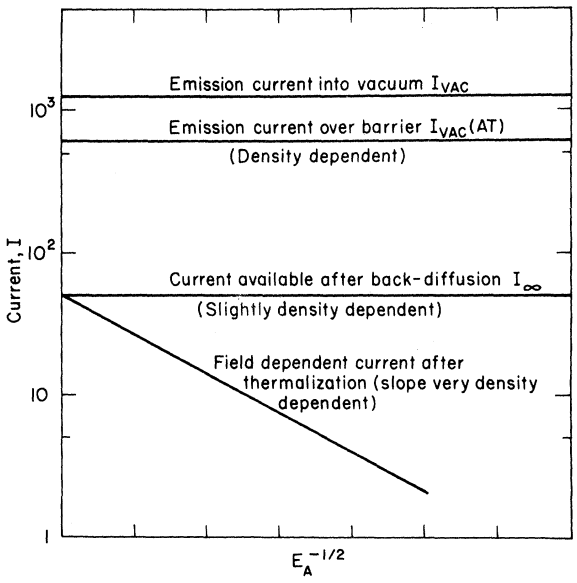

FIG. 6. Illustration of the effect of the current reduction terms contained in Eq. (20).

V. DISCUSSION

A. The i_c versus E_A Characteristics

Using the complete current equation [Eq. (20)] as a basis, we have replotted i_c versus E_A curves such as those shown earlier in Fig. 4. The complete results for one emitter are shown in Fig. 7, where i_c versus $E_A^{-1/2}$ is plotted for several operating voltages, v_d, at a variety of temperatures. This emitter was chosen for illustration because, being thick (~ 130 Å oxide) there is no need for aging corrections to be applied to the raw data, and it can be plotted directly. Similar characteristics have been obtained for a wide variety of emitters and although not all of them were operated over the entire range, the general features are repeated quite consistently. Data obtained from some other emitters will be used in the following discussion.

The general form of plots such as Fig. 7 agrees very well with the behavior expected from Eq. (20) represented schematically in Fig. 6. The change of temperature causes a change in liquid-helium density.

For a given v_d and temperature the data fit a straight line. The slope $d(\ln i_c)/dx_M$ will be $-1/x_0$. Values of x_M for the various field strengths used are shown along the uppermost abscissae. There are deviations from straight line behavior at the highest field strengths and temperatures used, but these may be due either to lack of thermal equilibrium, or to deviation from the conditions under which Eq. (20) was derived, under the high field close to the surface. Nevertheless, the constant slope of these plots over such a wide range of conditions provides a good measure of the thermalization range, x_0. The slope increases with decreasing temperature down to the λ point, but below the λ point the slope once more increases, though only slightly. The thermalization range, x_0, is decreasing with increasing helium density, to the λ point, but below the λ point, although x_0 again increases it does so more rapidly than the small density change would permit if the same scattering process applied. A plot of x_0 against reciprocal helium density is shown in Fig. 8 for three emitters. This is a development of an earlier plot[19] in which some of the higher temperature data was less reliable. It now appears that x_0 can be described by an equation of the form

$$x_0 = A/\rho + B\,, \tag{22}$$

where both the parameters A and B depend on the energy of the electrons (i.e., the emitter driving voltage). For the data shown in Fig. 8, the parameters for Eq. (22) are (A): 21 Å (gm cm^{-3}) for all three emitters and (B): − 80 Å (H-26); − 85 Å (H− 33); − 95 Å (H − 32).

Below the λ point, x_0 is increasing much more rapidly than in Eq. (22), indicating a change in the scattering mechanism in this region. Such a change is to be expected from the very different structure of helium above and below the λ point, but a careful study of the region below the λ point at lower temperatures than we have yet

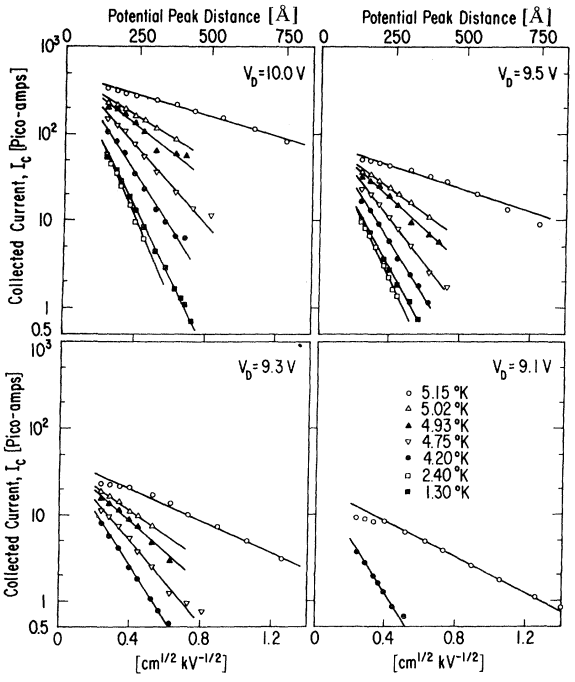

FIG. 7. Complete collected current data from one emitter. I_c is plotted against $(E_A)^{-1/2}$ for constant current operation of the emitter at four different driving voltages and at several temperatures for each voltage.

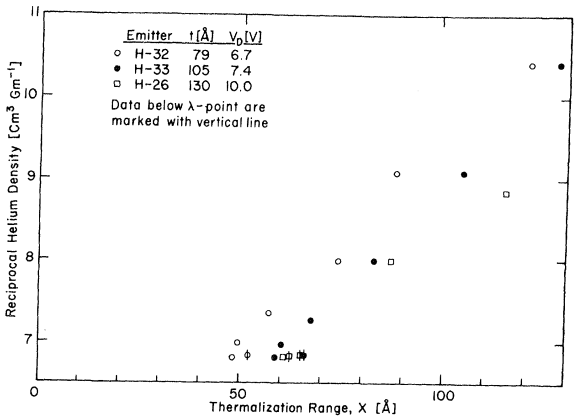

FIG. 8. Reciprocal density of liquid helium plotted against thermalization range (x_0) for three emitters operating at different peak driving voltages.

reached will be needed before any conclusions on the scattering mechanism can be drawn.

The data for a fixed v_d and temperature (Fig. 7) can be extrapolated to intercept the infinite field axis ($E_A^{-1/2} = 0$). The intercept represents the maximum amount of current that could be extracted from the emitter under infinite field conditions, and is identified from Eqs. (20) and (21) as I_∞. The possibility of such an extrapolation shows why one would not expect saturation of the collected current when the data is plotted as i_c versus E_A as in Fig. 4.

For a fixed v_d, the data for different temperatures extrapolate back very close to one point on the infinite field axis. Earlier data[19] indicated that there was one meeting point, but better fitting of the lines, together with later data from other emitters, shows a slight spread of the intercepts. Since I_{vac} is constant for fixed v_d, this spread must be due to a change in I_∞ with helium temperature. In general, (I_∞/I_{vac}) increases with decreasing temperature down to the λ point. Below the λ point (I_∞/I_{vac}) decreases rapidly again. It should be noted that the intercept, I_∞, is difficult to determine accurately due to the long extrapolation required, especially at the lower temperatures, where low currents, close to background, are measured. I_∞ is generally less accurately determined than x_0 for any line. However, we have obtained enough data on the various emitters operated to date, to show that the behavior of (I_∞/I_{vac}) described above is consistent. We have collected, in Table I, data from three emitters covering the widest temperature range. We compare (I_∞/I_{vac}) obtained experimentally with (I_a/I_{vac}) obtained from Thomson back diffusion, and thus estimate the effect of the term (AT) in Eq. (21).

In Table I, column 3 gives the experimentally determined values of (I_∞/I_{vac}). Column 4 is left blank to separate raw data from our interpretation. Column 5 gives the values of the thermalization range, x_0, obtained from Fig. 7 and similar plots. In column 6 we have used these values of x_0, together with the approximation that $x_x = x_s$, in Eq. (21) to calculate the current reduction due to back-diffusion, (I_a/I_{inj}). Finally, column 7 is the ratio of the experimental current reduction (column 3) to the back-diffusion term (column 6), and is thus the term (AT) in Eq. (21), since $(AT) = (I_{inj}/I_{vac})$.

The attenuation (AT) represents the effect of the electron-helium barrier, and from Table I it can be seen that (AT) varies in two ways that are compatible with the presence of such a bar-

TABLE I. Summary of results for three emitters (see text for explanation).

(1) Emitter and driving voltage	(2) T (°K)	(3) (I_∞/I_{vac})	(4)	(5) x_0 (Å)	(6) (I_a/I_{inj})	(7) (AT)	(8) τ (psec)
H-26	1.35	0.044		65	0.093	0.47	0.54
10.0 V	1.83	0.056		58	0.105	0.53	0.43
	2.38	0.052		57	0.106	0.49	0.42
	4.23	0.050		83	0.086	0.58	0.77
	4.76	0.047		115	0.071	0.66	1.5
	4.93	0.043		167	0.054	0.80	2.6
H-32	1.40	0.030		66	0.093	0.32	0.56
7.4 V	2.16	0.035		57	0.104	0.34	0.43
	2.74	0.038		60	0.102	0.37	0.46
	3.34	0.036		67	0.096	0.38	0.55
	4.23	0.042		84	0.086	0.48	0.78
	4.80	0.036		105	0.079	0.46	1.05
	5.05	0.039		128	0.074	0.53	1.39
H-33	1.40	0.014		52	0.115	0.21	0.35
6.7 V	2.16	0.025		48	0.121	0.21	0.30
	2.74	0.030		50	0.120	0.25	0.31
	3.34	0.033		57	0.110	0.30	0.40
	4.23	0.036		74	0.096	0.37	0.61
	4.80	0.041		86	0.094	0.44	0.71
	5.05	0.038		127	0.076	0.51	1.38

rier, dependent, as it is, on density of the liquid helium. First, for one emitter operating at constant driving voltage, (AT) increases with increasing temperature. Since the barrier decreases with increasing temperature (decreasing helium density), more electrons should be injected, and (AT) should increase. Second, for different emitters, operating at the same temperature, (AT) decreases with decreasing driving voltage. Figure 9 shows schematically why this should happen. The energy distributions are not intended to be exact, but have the features to be expected from previous work.[25-27] An emitter operated at driving voltage v_d, will have a distribution of emitted electrons up to an energy $(v_d - \phi_{Au})$. The barrier will cause a greater current reduction in the case of the low-voltage emitter than the high-voltage emitter, so that (AT) for the high-voltage emitter will be larger. The current marked as crosshatched in Fig. 9 will not be injected into the liquid helium at 4.8°K. The current shown shaded will not be injected at 2.2°K. The relative reduction in current agrees with Table I.

In summary, the main features of the collected current versus applied field data are compatible with the complete current equation [Eq. (20)], based on our model for injection. There remain two uncertainties that are unfortunately not separately determinable at the present. The use of x_S as the relevant mean free path to describe the scattering of the injected quasifree hot electrons gives uncertainty to the exact size of the back-diffusion term, and the lack of knowledge of the energy distribution of the injected electrons prevents quantitative calculations of the barrier transmission term (AT).

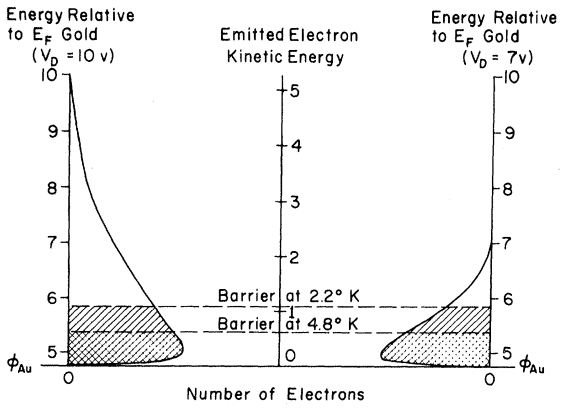

FIG. 9. Schematic showing the effect of the electron-helium barrier and its variation with temperature on the energy distribution of the current from two emitters with very different operating voltages.

B. Estimate of the Lifetime

In column 8 of Table I we have calculated the lifetime, τ, of the quasifree electrons before thermalization, according to Eq. (11), using for the electron velocity the value for electrons of 0.5-eV energy. Since $c \propto \epsilon^{1/2}$, where ϵ is the hot-electron kinetic energy after passing over the electron-helium barrier, the final value of τ is not very sensitive to the electron energy differences that may occur due to the changes in the barrier as the temperature changes.

The longest lifetime (2.5 psec) is obtained from the highest energy emitter (H-26) at the lowest helium densities. The lifetime decreases with both increasing helium density and decreasing electron energy.

Consideration of the nature of the current reduction terms provide good physical limits on the lifetime. We know that

$$I_\infty / I_{vac} = AT\,[1 + (6\pi)^{1/2} x_0 / x_x]^{-1} \qquad (21)$$

and

$$c\tau = 6x_0^2 / x_S \ . \qquad (11)$$

Discussing the particular case of H-26, $(I_\infty/I_{vac}) = 0.05$ at 4.2°K (Table I), is experimentally determined, as is x_0 (83 Å). Thus (AT) and x_X are essentially adjustable quantities as long as (I_∞/I_{vac}) is 0.05. But (AT) cannot be greater than unity, and if it were unity then the lowest possible value of x_X that agrees with the experimental current reduction is 4 Å. Calculating τ from Eq. (11) we thus obtain 2.5 psec as an upper limit on τ.

On the other hand, x_X cannot be greater than x_0. To obtain the experimentally determined current reduction (AT) would have to be 0.1 and τ about 0.1 psec. The upper and lower limits of 2.5 and 0.1 psec for electrons from H-26 should be compared with the value 0.77 psec obtained using $x_X = x_S$. The arguments used above give upper and lower limits on τ for all the operating conditions listed in Table I in the same range, i.e., upper and lower limits approximately three times and one tenth, respectively, of the tabulated value.

The only previous estimate of the thermalization time of a hot electron in liquid helium was made to estimate the formation time for a bubble.[1] The value obtained, 5 psec at 1.3°K, is slightly higher than the present estimates, but the temperature dependence would be similar. The difference may be explained by a more refined theoretical treatment of the entire thermalization process.

C. Source Dependence of x_0

Although it is not readily apparent due to the scale used in Fig. 7, there is a small change in

x_0 with v_d at a fixed temperature; thus the slopes of the lines at 4.2°K on the four separate sections of Fig. 7 do not quite agree. To show this more clearly, a smoothed plot has been made in Fig. 10, with the intercepts on the infinite field axis normalized to unity. From Fig. 10 it can be seen that the rate of change of x_0 with v_d is much more rapid for the thinner oxide, low-voltage emitter, which is expected to be a source of less energetic electrons. The data obtainable on any one emitter is limited by the short range of v_d for which currents in liquid helium are detectable, and the emitter still reliably operated.

To illustrate still further the dependence of x_0 on source conditions, the values of x_0 obtained for all reliable emitters operated to date are plotted in Fig. 11 as a function of driving voltage, v_d. Where the same symbols fall close together they indicate data on the same emitter at slightly different values of v_d. A separate grouping of the same symbol indicates a different emitter.

The variation of x_0 can be separated into two regions. For $v_d > 8$ V there is only a slight further increase in x_0 with increasing v_d, and for any one emitter, the rate of change of x_0 with v_d is greater than the overall trend. For $x_0 < 8$ V there is a much more marked dependence of x_0 on v_d, and the variation in one emitter agrees better with the overall trend. We can understand this difference qualitatively by reference to Fig. 9, remembering that the 10-V emitter is operated between 9 and 10 V and the 7-V emitter between 6 V and 7 V. Clearly the change of v_d on the 7-V emitter will have a much more marked effect on the average energy of the electrons passing over the barrier than will an equal change in the 10-V emitter. Unfortunately, it is very difficult to obtain reliable data from emitters that are thinner, or operated at lower voltages than the thinnest ones in Fig. 10, so that the low voltage behavior cannot yet be extrapolated to a zero-range condition.

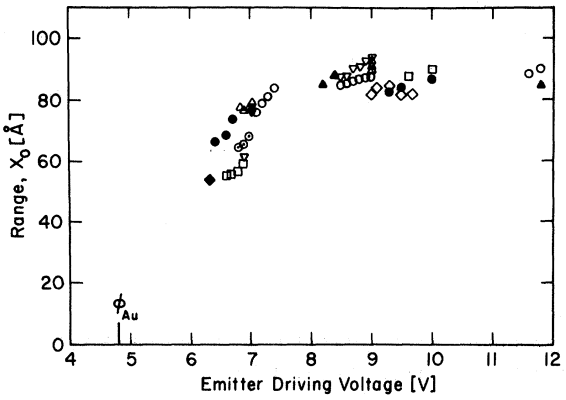

FIG. 11. Thermalization range x_0 plotted against driving voltage v_d for all emitters operated to data. Where the same symbols fall close together data is from one emitter. The same symbol elsewhere is for data from a different emitter. All data is at 4.2° K.

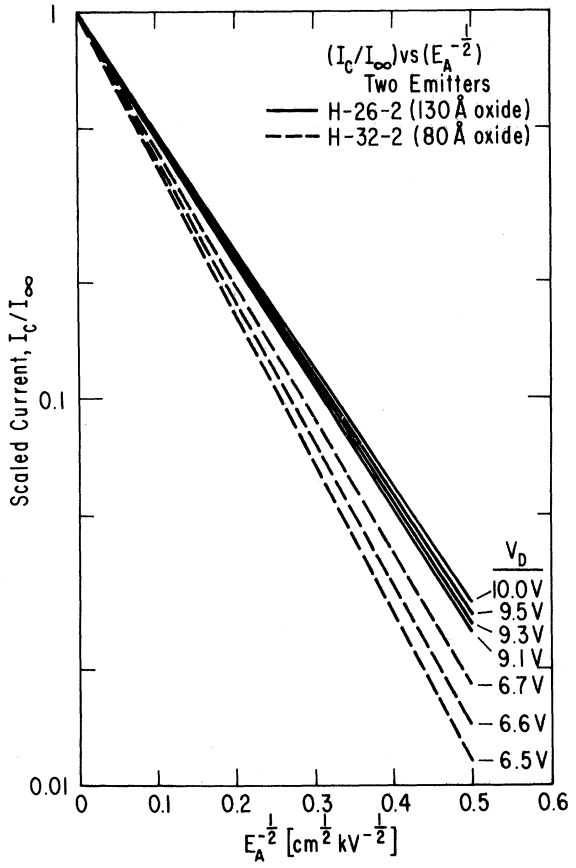

FIG. 10. Smoothed plot of reduced current (I_c/I_∞) against $E_A^{-1/2}$ showing the different slopes for two emitters, and the variation of slope for each emitter at different voltages.

D. The i_c versus $(1/v_d)$ Characteristics

We are now in a position to reexamine our earlier interpretation[18] of the slope change of the [i_c versus $(1/v_d)$] characteristics (Fig. 3). Due to the variety of factors affecting the slope of the helium data we cannot interpret the slope difference between helium and vacuum lines as due only to a work function change caused by the presence of the electron-helium barrier. Comparison can only be made between the vacuum line and helium data taken under infinite applied field conditions, or extrapolated to infinite applied field conditons. Even then we have seen that the extrapolated current value (I_∞) is not a simple function of the electron helium barrier. We have at-

tempted to obtain (I_∞/I_{vac}) as a function of v_d for several emitters, but the uncertainty in the extrapolation to infinite field conditions increases as v_d decreases, preventing us from drawing any firm conclusions at present.

VI. SUMMARY AND CRITICISMS

We have studied the reduction of a current emitted from the gold surface of a cold cathode into liquid helium below the current emitted into a vacuum. The current reduction can be explained in terms of a model involving three main sources of attenuation: (a) the electron-helium barrier at the gold surface, combined with a possible transmission coefficient change between gold-vacuum and gold-helium surfaces; (b) the back diffusion of the quasifree nonlocalized hot electrons that have been injected over the barrier into the liquid helium, but are not yet thermalized to the bubble state; (c) a thermalization process for the hot electrons which we characterize by a range x_0 and a time τ, occurring in the region close to the emitter, where thermalized electrons may not have passed beyond the influence of their image force due to the gold surface.

We have deduced an equation for the collected current [Eq. (20)] after these three processes have been estimated, and have shown experimentally that the dependence of the collected current on the electric field applied to the helium, and the helium density, are compatible with this equation. Lack of information on either the relevant mean free path to describe the scattering process of the hot electrons, or the energy distribution of the emitted electrons requires the approximation that the mean free path to be used is that for elastic scattering of the hot electrons. Using this approximation we have calculated the lifetime τ of the hot electrons before thermalization, and the dependence of τ on the helium density. Physical arguments enable us to set upper and lower limits on τ, the upper limit being only slightly lower than the time for bubble formation based on the time for a bubble to be formed if the helium atoms move at their thermal velocity.

The present model is intended as a plausible physical picture of the injection of hot electrons into liquid helium. A major question arises over the energy dissipation mechanism for the hot electrons, and the final process by which the electron becomes thermalized, or forms a bubble. A more detailed theoretical study of this step in the injection process would be very useful.

We do not have enough data to draw any firm conclusions about behavior below the λ point, but the absence of any marked discontinuity in the injected current attenuation implies that the injection process is not greatly different below the λ point. However, the increasing range of the electrons with decreasing temperature below the λ point suggests that the scattering mechanism for the hot electrons is different.

The use of this type of cold-cathode emitter as a source of electrons in liquid helium has the advantage over the usual radioactive sources, that the emission is certainly only electrons, and is controllable at the source, rather than by a grid system. However, there is a disadvantage in that very high applied fields in the helium are required in order to obtain the same current into helium as is provided by other sources. We obtained up to 10^{-9} A cm^{-2} injected current, but only with a field of 20 kV cm^{-1} applied to the liquid helium.

Further interpretation of our data is limited at present by lack of knowledge of the energy distributions of the emitted electrons. We are currently studying these distributions and continuing work on injection into liquid helium and other liquids.[35]

[1]R. A. Ferrel, Phys. Rev. 108, 167 (1957).
[2]C. G. Kuper, Phys. Rev. 122, 1007 (1961).
[3]K. Hiroike, N. R. Kestner, S. A. Rice, and J. Jortner, J. Chem. Phys. 43, 2625 (1965).
[4]J. L. Levine and T. M. Sanders, Phys. Rev. 154, 138 (1967).
[5]J. Jortner and S. A. Rice, Progress in Dielectrics, edited by J. B. Birks and J. Hart (Academic Press Inc., New York, 1965), Vol. 6, p. 185.
[6]R. W. LaBahn and J. Callaway, Phys. Rev. 135, A1539 (1964).
[7]T. F. O'Malley, Phys. Rev. 130, 1020 (1965).
[8]N. R. Kestner, J. Jortner, M. H. Cohen, and S. A. Rice, Phys. Rev. 140, A56 (1965).
[9]D. E. Golden and H. W. Bandel, Phys. Rev. 138, A14 (1965).
[10]R. C. Clark, Phys. Rev. Letters 16, 42 (1965).
[11]P. E. Parks and R. J. Donnelly, Phys. Rev. Letters 16, 45 (1966).
[12]J. A. Northby and T. M. Sanders, Phys. Rev. Letters 18, 1184 (1967).
[13]C. V. Briscoe, S.-I Choi, and A. T. Stewart, Phys. Rev. Letters 20, 493 (1968).
[14]B. Burdick, Phys. Rev. Letters 14, 11 (1965).
[15]W. T. Sommer, Phys. Rev. Letters 12, 271 (1964).
[16]M. A. Woolf and G. W. Rayfield, Phys. Rev. Letters 15, 235 (1965).
[17]C. Zipfel and T. M. Sanders, in Proceedings of the Eleventh International Low Temperature Physics Conference (St. Andrews University Press, St. Andrews,

Scotland 1968).
[18]M. Silver, D. G. Onn, P. Smejtek, and K. Masuda, Phys. Rev. Letters 19, 626 (1967).
[19]M. Silver and D. G. Onn, in Proceedings of the Eleventh International Low Temperature Physics Conference, (St. Andrews University Press, St. Andrews, Scotland 1968).
[20]C. A. Mead, J. Appl. Phys. 32, 4, 646 (1961).
[21]C. R. Crowell and S. M. Sze, Physics of Thin Films, edited by G. Hass and R. E. Thun (Academic Press Inc., New York, 1967), Vol. 4, p. 350.
[22]E. D. Savoye and D. E. Anderson, J. Appl. Phys. 38, 3245 (1967).
[23]G. Haas, J. Opt. Soc. Am. 39, 532 (1949).
[24]R. M. Handy, Phys. Rev. 126, 1968 (1962).
[25]D. G. Onn, P. Smejtek, and M. Silver (to be published).
[26]J. S. Vinson, F. J. Agee, R. J. Manning, and F. L. Hereford, Phys. Rev. 167, 180 (1968).
[27]R. E. Collins and L. W. Davies, Solid State Electron. 7, 445 (1964).
[28]F. C. Witteborn and W. M. Fairbank, Phys. Rev. Letters 19, 1049 (1967).
[29]R. M. Handy, J. Appl. Phys. 37, 4620 (1966).
[30]Y. Mentalechata, G. Delacote, and M. Schott, Compt. Rend. 262, 892 (1966) and Y. Mentalechata, Ph. D. thesis, Université d'Alger, 1967 (unpublished).
[31]J. Bardeen, Phys. Rev. 49, 653 (1936); and 58, 727 (1940).
[32]J. J. Thomson and G. P. Thomson, Conduction of Electricity Through Gases (Cambridge University Press, London, England, 1928), 3rd ed., Vol. 1, p. 466.
[33]M. H. Cohen and J. Lekner, Phys. Rev. 158, 305 (1967).
[34]L. J. Challis, K. Dransfeld, and J. Wilks, Proc. Roy. Soc. (London) A260, 31 (1961).
[35]M. Silver, P. Smejtek, D. G. Onn, and S.-I. Choi, J. Appl. Phys. (to be published).

PHYSICAL REVIEW VOLUME 183, NUMBER 1 5 JULY 1969

Instability of Two-Electron Bubbles and Bubble Formation in Liquid Helium*

D. L. Dexter
Department of Physics and Astronomy, University of Rochester, Rochester, New York 14627
and
W. Beall Fowler
Department of Physics, Lehigh University, Bethlehem, Pennsylvania 10815
(Received 3 February 1969)

The energy of a two-electron bubble in liquid He is computed with a correlated electronic wave function. Without correlation the bubble is unstable against decay into two one-electron bubbles; correlation reduces the energy by about $\frac{1}{2}$ eV, but the bubble is still unstable. However, a free electron can be trapped by a one-electron bubble. The resulting metastable bubble will expand and presumably split into two bubbles. Experiments are suggested to test the trapping and splitting hypotheses.

In addition to their practical utility as a probe of excitations of liquid helium, electronic bubbles are of intrinsic interest for their own unusual properties.[1] The bubble seems now to be established as a spherical cavity of some 15 Å radius stabilized by the zero-point kinetic energy of an electron contained therein. The low polarizability (hence low surface tension) of helium, and the large Pauli principle repulsion of helium for an electron makes this the lowest-energy configuration for an additional electron introduced into the liquid. To our knowledge the mechanism of formation of these bubbles has not been elucidated.

We recently made a theoretical spectroscopic study[2] of bubbles, and in passing estimated that a two-electron bubble would be unstable against decay into two one-electron bubbles by an energy of the order 1 eV. However, a one-electron bubble has a remarkably high electronic polarizability, $\alpha = 0.876 \times 10^{-20}$ cm^3, some 4.4×10^4 times higher than that of a He atom, or 89 times higher than the 500 atoms it displaces. It seemed that a more accurate analysis of two-electron bubbles was warranted. The results, while confirming the nonstability of two-electron bubbles,